

University of Nebraska - Lincoln

DigitalCommons@University of Nebraska - Lincoln

Faculty Publications from the Department of
Electrical and Computer Engineering

Electrical & Computer Engineering, Department of

2015

CMI analysis and precoding designs for correlated multi-hop MIMO channels

Nguyen N. Tran

Vietnam National University, nntran@fetel.hcmus.edu.vn

Song Ci

University of Nebraska-Lincoln, sci2@unl.edu

Ha X. Nguyen

Tan Tao University

Follow this and additional works at: <http://digitalcommons.unl.edu/electricalengineeringfacpub>



Part of the [Computer Engineering Commons](#), and the [Electrical and Computer Engineering Commons](#)

Tran, Nguyen N.; Ci, Song; and Nguyen, Ha X., "CMI analysis and precoding designs for correlated multi-hop MIMO channels" (2015). *Faculty Publications from the Department of Electrical and Computer Engineering*. 395.
<http://digitalcommons.unl.edu/electricalengineeringfacpub/395>

This Article is brought to you for free and open access by the Electrical & Computer Engineering, Department of at DigitalCommons@University of Nebraska - Lincoln. It has been accepted for inclusion in Faculty Publications from the Department of Electrical and Computer Engineering by an authorized administrator of DigitalCommons@University of Nebraska - Lincoln.

RESEARCH

Open Access

CMI analysis and precoding designs for correlated multi-hop MIMO channels

Nguyen N Tran^{1*}, Song Ci² and Ha X Nguyen³

Abstract

Conditional mutual information (CMI) analysis and precoding design for generally correlated wireless multi-hop multi-input multi-output (MIMO) channels are presented in this paper. Although some particular scenarios have been examined in existing publications, this paper investigates a generally correlated transmission system having spatially correlated channel, mutually correlated source symbols, and additive colored Gaussian noise (ACGN). First, without precoding techniques, we derive the optimized source symbol covariances upon mutual information maximization. Secondly, we apply a precoding technique and then design the precoder in two cases: maximizing the mutual information and minimizing the detection error. Since the optimal design for the end-to-end system cannot be analytically obtained in closed form due to the non-monotonic nature, we relax the optimization problem and attain sub-optimal designs in closed form. Simulation results show that without precoding, the average mutual information obtained by the asymptotic design is very close to the one obtained by the optimal design, while saving a huge computational complexity. When having the proposed precoding matrices, the end-to-end mutual information significantly increases while it does not require resources of the system such as transmission power or bandwidth.

Keywords: Precoding design; MIMO spatially correlated channel; Mutual information and channel capacity; Multi-hop relay network; Colored noise

1 Introduction

With the fast-paced development of computing technologies, wireless devices have enough computation and communication capabilities to support various multimedia applications. To deliver high-quality multimedia over a wireless channel, multi-input multi-output (MIMO) technology has been emerging as one of the enabling technologies for the next-generation multimedia systems by providing very high-speed data transmission over wireless channels [1]. In the last decade, MIMO has been adopted by almost all new LTE, 3GPP, 3GPP2, and IEEE standards for wireless broadband transmission to support wireless multimedia applications [2-7]. A fundamental assumption of MIMO system design is placing antennas far enough [3] from each other to make fading uncorrelated. It means that different pairs of transmitting and receiving antennas are uncorrelated so that the channel statistical knowledge can be expressed as a diagonal covariance matrix.

However, this assumption is no longer held true for compact embedded multimedia system design due to the small form factor. The compact system design will cause a MIMO spatial correlation problem [8-13], leading to a significant deterioration on the system performance. Furthermore, the pervasive use of computing devices such as laptop computers, PDAs, smart phones, automotive computing devices, wearable computers, and video sensors leads to a fast-growing deployment of wireless mesh networks (WMN) [14] to connect these computing devices by a multi-hop wireless channel. Therefore, how to achieve high channel capacity by using multi-hop MIMO transceivers under strict space limitations is the fundamental question targeted in this paper.

In the first part of this paper, we analyze the capacity (or bound on the capacity) of generally correlated wireless multi-hop amplify-and-forward (AF) MIMO channels. For generality, we consider a wireless system, in which the channel at each hop is spatially correlated but independent of that at the other hops, the source symbols are mutually correlated, and the additive Gaussian noises are colored. Although most previous works on wireless

*Correspondence: nntran@fetel.hcmus.edu.vn

¹ Faculty of Electronics and Telecommunications, University of Science, Vietnam National University, Ho Chi Minh City, Vietnam
Full list of author information is available at the end of the article

channel only consider *white* noise and *uncorrelated* data symbols, the assumption of white noise is not always true (see, e.g., [15–19]). Moreover, in practice, the case of correlated data symbols arises due to various signal processing operations at the baseband in the transmitter.

For less than three-hop wireless channel, various works have been done on the capacity or bounds on the capacity [1, 13, 20–24]. For multi-hop relay network, capacity analysis was proposed in [25–27]. In [25], the authors considered rate, diversity, and network size in the analysis. In [26, 27], the authors assumed that there is no noise at relay nodes, and the number of antennas is very large. Since these assumptions are not feasible in compact MIMO design with mutual interference, in this paper, we consider a generally correlated system at the wireless fading channel, data symbols, and additive colored Gaussian noises (ACGN). It includes the correlated system assumption in [26, 27] as a special case. First, we derive the optimal source symbol covariance to maximize the mutual information between the channel input and the channel output when having the full knowledge of channel at the transmitters. Secondly, the numerical interior point method-based solution and an asymptotic solution in closed form are derived to maximize the average mutual information when having only the channel statistics at the transmitters. Although the asymptotic design is very simple and comes by maximizing an upper bound of the objective function, simulation results show that the asymptotic design performs well as the numerically optimal design.

In the second part of this paper, we apply the precoding technique and then design the precoding matrix to either maximizing the mutual information or minimizing the detection error. It has been shown in [20] that beamforming, which can be considered as a particular case of precoding, increases the mutual information of single-hop MIMO channel. In [28], the outage capacity of multi-hop MIMO networks is investigated, and the performance of several relaying configurations and signaling algorithms is discussed. In [25], the authors considered rate, diversity, and network size in the analysis. The multi-hop capacity of OFDM-based MIMO-multiplexing relaying systems is derived in [29, 30] for frequency-selective fading channels. Apparently, in the literature, only references [26, 27] actually study the asymptotic capacity and precoding design for wireless correlated multi-hop MIMO relay networks. Under a special case of wireless channels having only white noise at the destination, no noise at all relay levels, and the number of antennas is very large (to infinity); references [26, 27] provide the precoding strategy and asymptotic capacity. Since the special wireless channel assumption in [26, 27] is not always feasible for compact MIMO design with space limitation and mutual interference at various signal-to-noise ratio (SNR)

levels, in this paper, we design precoders for the generally correlated AF system. Obviously, the optimal capacity and precoding design cannot be analytically obtained in closed form as the design problem is very complicated and neither convex nor concave. Similarly to [26, 27], for generally correlated multi-hop MIMO channels, we propose asymptotic designs in closed form.

First, instead of designing the optimal precoding strategy to maximize the end-to-end mutual information, we derive the sub-optimal precoding strategy by optimally maximizing the mutual information between the input and output signals at each hop. Since the mutual information and detection error have a very close relationship, we further propose the other sub-optimal precoding strategy by optimally minimizing the mean square error (MSE) of the soft detection of the transmitted signal at each hop. Simulation results show that the asymptotic precoding designs are efficient. They significantly increase the end-to-end mutual information, while do not require any resource of the system such as transmission power or bandwidth.

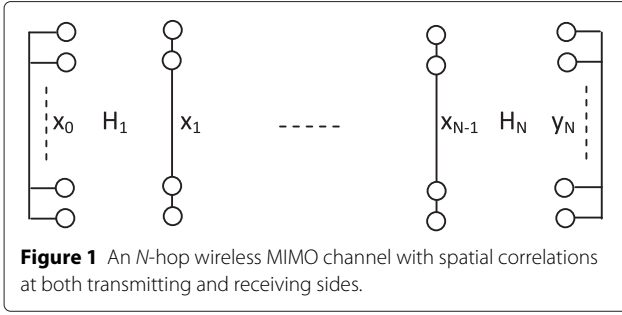
The paper is organized as follows. Section 2 first describes the correlated wireless multi-hop MIMO model without any precoding techniques and then designs the source signal covariance to maximize the mutual information in two cases: having full knowledge of channel state information at the transmitters and having only the channel statistics at the transmitters. Section 3 first proposes the precoding design to maximize the mutual information and then proposes the precoding design to minimize the soft detection error. Simulation results are provided in Section 4 and Section 5 concludes the paper.

Notation: Boldface upper and lower cases denote matrices and column vectors. Superscript $*$ and H depict the complex conjugate and the Hermitian adjoint operator, while \otimes stands for the Kronecker product. \mathbf{I}_N is the $N \times N$ identity matrix. Sometimes, the index N are omitted when the size of the identity matrix is clear in the context. $E\{z\}$ is the expectation of the random variable z and $\text{tr}\{\mathbf{A}\}$ is the trace of the matrix \mathbf{A} . $\mathcal{I}(\cdot)$ and $\mathcal{H}(\cdot)$ denote the mutual information and the entropy, respectively. \mathbf{R}_{xy} depicts the covariance matrix of two random variables x and y . $\mathbf{A} \leq \mathbf{B}$ ($\mathbf{A} < \mathbf{B}$, respectively) for symmetric matrices \mathbf{A} and \mathbf{B} means that $\mathbf{B} - \mathbf{A}$ is a positive semi-definite (definite, respectively) Hermitian matrix.

2 The correlated channel and mutual information maximization

2.1 Spatially correlated wireless multi-hop MIMO channel

Consider an N -hop wireless MIMO channel as presented in Figure 1. The MIMO system has a_0 antennas at the source, a_i antennas at the i -th relay, and a_N antennas at the destination. Then, the channel gain matrix at the i -th



hop is represented by the Kronecker model [11,12,31-35] as:

$$\mathbf{H}_i = \boldsymbol{\Sigma}_{ri}^{1/2} \mathbf{H}_{wi} \boldsymbol{\Sigma}_{ti}^{1/2} \in \mathbb{C}^{a_i \times a_{i-1}}, i = 1, \dots, N,$$

where

$$\mathbf{H}_i = \begin{bmatrix} h_{11}(i) & \dots & h_{1a_{i-1}}(i) \\ \vdots & \dots & \vdots \\ h_{a_i1}(i) & \dots & h_{a_i a_{i-1}}(i) \end{bmatrix},$$

and $\boldsymbol{\Sigma}_{ti}$ and $\boldsymbol{\Sigma}_{ri}$ are $a_{i-1} \times a_{i-1}$ and $a_i \times a_i$ known covariance matrices that capture the correlations of the transmitting and receiving antenna arrays, respectively. The matrix \mathbf{H}_{wi} is an $a_i \times a_{i-1}$ matrix whose entries are independent and identically distributed (i.i.d.) circularly symmetric complex Gaussian random variables of variance σ_{hi}^2 , i.e., $\mathcal{CN}(0, \sigma_{hi}^2)$. The known matrices $\boldsymbol{\Sigma}_{ri}$ and $\boldsymbol{\Sigma}_{ti}$ are assumed to be invertible and have the following forms:

$$\boldsymbol{\Sigma}_{ti} = \begin{bmatrix} 1 & t_{12}(i) & \dots & t_{1a_{i-1}}(i) \\ t_{12}^*(i) & 1 & \dots & t_{2a_{i-1}}(i) \\ \vdots & \vdots & \ddots & \vdots \\ t_{1a_{i-1}}^*(i) & t_{2a_{i-1}}^*(i) & \dots & 1 \end{bmatrix},$$

$$\boldsymbol{\Sigma}_{ri} = \begin{bmatrix} 1 & r_{12}(i) & \dots & r_{1a_i}(i) \\ r_{12}^*(i) & 1 & \dots & r_{2a_i}(i) \\ \vdots & \vdots & \ddots & \vdots \\ r_{1a_i}^*(i) & r_{2a_i}^*(i) & \dots & 1 \end{bmatrix}, \quad (1)$$

where t_{ij} (r_{nm} , respectively) with $i \neq j$ ($n \neq m$, respectively) reflects the correlated fading between the i -th and the j -th (n -th and m -th, respectively) elements of the transmitting (receiving, respectively) antenna array. The channel at each hop undergoes correlated MIMO Rayleigh flat fading. However, the fading channels of any two different hops are independent. Moreover, the channel at each hop is quasi-static block fading with a suitable coherence time for the system to be in the non-ergodic regime.

The ACGN at i -th hop is defined as \mathbf{n}_i with zero-mean and covariance matrix $\mathbb{E}\{\mathbf{n}_i \mathbf{n}_i^H\} = \mathbf{R}_i$, $i = 1, \dots, N$. Additionally, $\mathbf{n}_1, \dots, \mathbf{n}_N$ are all independent of each other, i.e., the colored noise at each hop is statistically uncorrelated with the colored noise at the other hops.

The vector \mathbf{x}_0 that contain the data symbols at the source is modeled as complex random variables with covariance matrix $\mathbf{R}_{x_0} = \mathbb{E}\{\mathbf{x}_0 \mathbf{x}_0^H\}$ under the power constraint $\text{tr}\{\mathbf{R}_{x_0}\} = P_0$. For the general case of correlated data symbols, $\mathbf{R}_{x_0} \neq \beta \mathbf{I}_{a_0}$, $\beta > 0$, while $\mathbf{R}_{x_0} = \mathbb{E}\{\mathbf{x}_0 \mathbf{x}_0^H\} = \beta \mathbf{I}_{a_0}$ for the case of uncorrelated data symbols.

Accordingly, the received signal at the destination can be expressed as:

$$\begin{aligned} \dot{\mathbf{y}}_N &= \mathbf{H}_N \mathbf{H}_{N-1} \dots \mathbf{H}_2 \mathbf{H}_1 \mathbf{x}_0 + \mathbf{n}_N + \mathbf{H}_N \mathbf{n}_{N-1} \\ &\quad + \mathbf{H}_N \mathbf{H}_{N-1} \mathbf{n}_{N-2} + \dots + \mathbf{H}_N \mathbf{H}_{N-1} \dots \mathbf{H}_2 \mathbf{n}_1. \end{aligned} \quad (2)$$

Let

$$\mathbf{G}_N = \mathbf{H}_N \mathbf{H}_{N-1} \dots \mathbf{H}_2 \mathbf{H}_1$$

be the end-to-end equivalent channel, and

$$\begin{aligned} \dot{\mathbf{n}} &= \mathbf{n}_N + \mathbf{H}_N \mathbf{n}_{N-1} + \mathbf{H}_N \mathbf{H}_{N-1} \mathbf{n}_{N-2} + \dots \\ &\quad + \mathbf{H}_N \mathbf{H}_{N-1} \dots \mathbf{H}_2 \mathbf{n}_1 \end{aligned}$$

be the end-to-end equivalent noise with the noise covariance matrix being

$$\begin{aligned} \mathbf{R}_{\dot{\mathbf{n}}} &= \mathbb{E}\{\dot{\mathbf{n}} \dot{\mathbf{n}}^H\} \\ &= \mathbf{R}_N + \mathbf{H}_N \mathbf{R}_{N-1} \mathbf{H}_N^H + \mathbf{H}_N \mathbf{H}_{N-1} \mathbf{R}_{N-2} \mathbf{H}_{N-1}^H \mathbf{H}_N^H + \dots \\ &\quad + \mathbf{H}_N \dots \mathbf{H}_2 \mathbf{R}_1 \mathbf{H}_2^H \dots \mathbf{H}_N^H. \end{aligned} \quad (3)$$

Therefore, Equation 2 can be rewritten as:

$$\dot{\mathbf{y}}_N = \mathbf{G}_N \mathbf{x}_0 + \dot{\mathbf{n}}. \quad (4)$$

2.2 Mutual information maximization and channel capacity when having channel state information at the transmitters

The conditional mutual information (CMI) [36] between the transmitted signal \mathbf{x}_0 and the received signal $\dot{\mathbf{y}}_N$ in Equation 4 is given by:

$$\mathcal{I}(\mathbf{x}_0; \dot{\mathbf{y}}_N) = \mathcal{H}(\mathbf{x}_0) - \mathcal{H}(\mathbf{x}_0 | \dot{\mathbf{y}}_N) \quad (5)$$

$$= \mathcal{H}(\dot{\mathbf{y}}_N) - \mathcal{H}(\dot{\mathbf{y}}_N | \mathbf{x}_0). \quad (6)$$

For the MIMO channel in Equation 4, the capacity is defined as [36]:

$$C = \max_{p(\mathbf{x})} \mathcal{I}(\mathbf{x}_0; \dot{\mathbf{y}}_N), \quad (7)$$

where $p(\mathbf{x})$ is the probability mass function (PMF) of the random variable \mathbf{x}_0 . The maximum is taken over all possible input distributions $p(\mathbf{x})$.

Note that we have the fundamental condition [37] $\det(\mathbf{I} + \mathbf{XY}) = \det(\mathbf{I} + \mathbf{YX})$. By Theorem 3 and Theorem 4 in the Appendix, the CMI in Equation 6 can be expressed as:

$$\begin{aligned} \mathcal{I}(\mathbf{x}_0; \dot{\mathbf{y}}_N) &= \mathcal{H}(\mathbf{x}_0) - \mathcal{H}(\mathbf{x}_0 | \dot{\mathbf{y}}_N) \\ &= \log \det(\pi e \mathbf{R}_{x_0}) \\ &\quad - \log \det \left[\pi e \left(\mathbf{R}_{x_0} - \mathbf{R}_{\dot{\mathbf{y}}_N x_0}^T \mathbf{R}_{\dot{\mathbf{y}}_N}^{-1} \mathbf{R}_{\dot{\mathbf{y}}_N x_0} \right) \right] \\ &= \log \det \left(\mathbf{I} + \mathbf{R}_{x_0} \mathbf{G}_N^H \mathbf{R}_n^{-1} \mathbf{G}_N \right) \\ &= \log \det \left(\mathbf{I} + \mathbf{R}_n^{-1} \mathbf{G}_N \mathbf{R}_{x_0} \mathbf{G}_N^H \right). \end{aligned} \quad (8)$$

To obtain the channel capacity, we now design the transmitted signal covariance to maximize the mutual information in Equation 8:

$$\max_{\mathbf{R}_{x_0} \geq 0, \text{tr}(\mathbf{R}_{x_0}) \leq P_0} \log \det \left(\mathbf{I} + \mathbf{R}_{x_0} \mathbf{G}_N^H \mathbf{R}_n^{-1} \mathbf{G}_N \right), \quad (10)$$

under the allowed transmitted signal power P_0 . For simple cases of channel characteristics, the solution of Equation 10 can be derived from the Hadamard inequality argument [36]. We now give a direct solution method based on spectral optimization for the general case.

Let $\mathbf{Q} = \mathbf{R}_{x_0} \geq 0$ and $\mathbf{P} = \mathbf{G}_N^H \mathbf{R}_n^{-1} \mathbf{G}_N > 0$. Equation 10 can be written as:

$$\max_{\mathbf{Q} \geq 0, \text{tr}(\mathbf{Q}) \leq P_0} \log \det(\mathbf{I} + \mathbf{QP}), \quad (11)$$

where its optimal solution \mathbf{Q} can be obtained in closed form by the following theorem.

Theorem 1. *The optimal solution \mathbf{Q} to the maximization problem*

$$\max_{\mathbf{Q} \geq 0, \text{tr}(\mathbf{Q}) \leq P_0} \log \det(\mathbf{I} + \mathbf{QP}), \quad (12)$$

is $\mathbf{Q} = \mathbf{U}^H \mathbf{D}_p^{-1} \mathbf{X} \mathbf{U}$. Here, \mathbf{U} is the unitary matrix obtained from the singular value decomposition (SVD) of $\mathbf{P} = \mathbf{U}^H \mathbf{D}_p \mathbf{U}$, and \mathbf{X} is the diagonal matrix having its diagonal elements $X(i, i)$ satisfy:

$$D_p^{-1}(i, i) X(i, i) = (\mu^{-1} - D_p^{-1}(i, i))^+, \quad (13)$$

where $x^+ = \max\{0, x\}$ and μ is chosen such that $\text{Trace}(\mathbf{D}_p^{-1} \mathbf{X}) = P_0$.

Proof of Theorem 1. : See Appendix.

2.3 Average mutual information maximization and channel capacity with only the channel statistics at the transmitters

The end-to-end mutual information between the transmitted signal \mathbf{x}_0 and received signal $\dot{\mathbf{y}}_N$ in Equation 4

is given by Equation 6. When considering the mutual information for a long time period, the average end-to-end mutual information between channel input \mathbf{x}_0 and channel output $(\dot{\mathbf{y}}_N, \mathbf{G}_N)$ can be expressed as:

$$\mathcal{I}(\mathbf{x}_0; (\dot{\mathbf{y}}_N, \mathbf{G}_N)) = \mathbb{E}_{\mathbf{G}_N} \left\{ \log \det \left(\mathbf{I} + \mathbf{R}_{x_0} \mathbf{G}_N^H \mathbf{R}_n^{-1} \mathbf{G}_N \right) \right\}.$$

Under the transmitted power constraint P_0 , we have to solve the this optimization problem:

$$\max_{\mathbf{R}_{x_0} \geq 0, \text{tr}(\mathbf{R}_{x_0}) \leq P_0} \mathbb{E}_{\mathbf{G}_N} \left\{ \log \det \left(\mathbf{I} + \mathbf{R}_{x_0} \mathbf{G}_N^H \mathbf{R}_n^{-1} \mathbf{G}_N \right) \right\} \quad (14)$$

to obtain the capacity in the non-ergodic regime of the system. Since the objective function is the expectation of a concave function with respect to the to-be-designed variable, obtaining the optimal solution in closed form to this problem is very difficult or almost impossible. We propose to use ‘SeDuMi’ [38] or ‘SDPT 3’ [39] solver for a numerically optimal solution. To reduce the computational complexity, an asymptotic solution in closed form is also derived by relaxing the objective function.

Since the function $\mathbf{R}_{x_0} \rightarrow \log \det \left(\mathbf{I} + \mathbf{R}_{x_0} \mathbf{G}_N^H \mathbf{R}_n^{-1} \mathbf{G}_N \right)$ is concave, it is obvious that:

$$\begin{aligned} \mathbb{E}_{\mathbf{G}_N} \left\{ \log \det \left(\mathbf{I} + \mathbf{R}_{x_0} \mathbf{G}_N^H \mathbf{R}_n^{-1} \mathbf{G}_N \right) \right\} \\ \leq \log \det \left(\mathbf{I} + \mathbb{E}_{\mathbf{G}_N} \left\{ \mathbf{R}_{x_0} \mathbf{G}_N^H \mathbf{R}_n^{-1} \mathbf{G}_N \right\} \right). \end{aligned}$$

Therefore, instead of maximizing the average end-to-end mutual information between the channel input and channel output, we now maximize an upper bound of the mutual information. Simulation results will show that this upper bound is closed to the true mutual information value. The relaxed optimization problem is now expressed as:

$$\max_{\mathbf{R}_{x_0} \geq 0, \text{tr}(\mathbf{R}_{x_0}) \leq P_0} \log \det \left(\mathbf{I} + \mathbf{R}_{x_0} \mathbb{E}_{\mathbf{G}_N} \left\{ \mathbf{G}_N^H \mathbf{R}_n^{-1} \mathbf{G}_N \right\} \right). \quad (15)$$

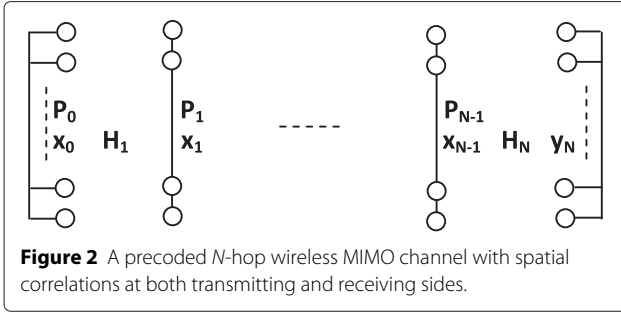
Again, let $\mathbf{Q} = \mathbf{R}_{x_0} \geq 0$ and $\mathbf{P} = \mathbb{E}_{\mathbf{G}_N} \left\{ \mathbf{G}_N^H \mathbf{R}_n^{-1} \mathbf{G}_N \right\} > 0$, it can be seen that Problem (15) is now in the form of (11), and hereby, the solution to (15) can be optimally obtained.

3 Precoding design for spatially correlated wireless multi-hop MIMO channel

3.1 Precoded N -hop wireless MIMO channel formulation

By applying the precoding technique to the wireless system, a precoded N -hop wireless MIMO channel is presented in Figure 2. Before transmitting over the wireless channel, the source signal \mathbf{x}_0 is linearly precoded by a linear precoder \mathbf{P}_0 such that the transmitted signal at the source is:

$$\bar{\mathbf{x}}_0 = \mathbf{P}_0 \mathbf{x}_0, \quad \mathbf{P}_0 \in \mathbb{C}^{a_0 \times a_0}.$$



For the sake of saving transmission bandwidth, all precoding matrices considered in this paper are square, i.e., non-redundancy precoder. The purpose of precoding technique here is to re-form the transmitted signal and re-allocate the transmitted power such that the transmitted signal can effectively combat the spatial correlation and colored noise in the eigen-mode. For single-hop wireless channels, the non-redundancy precoders to cope with spatial correlations and colored noises have been successfully proposed in [35,40] and in [19], respectively.

The received signal at the first hop can be expressed as:

$$\mathbf{x}_1 = \mathbf{H}_1 \bar{\mathbf{x}}_0 + \mathbf{n}_1 = \mathbf{H}_1 \mathbf{P}_0 \mathbf{x}_0 + \mathbf{n}_1.$$

Since the AF strategy is considered, the received signal \mathbf{x}_i at the i -th hop is also the source signal at the next hop. Before transmitting over the wireless channel, the source signal \mathbf{x}_i is also linearly precoded by a linear precoder \mathbf{P}_i such that the transmitted signal at the i -th transmitter is:

$$\bar{\mathbf{x}}_i = \mathbf{P}_i \mathbf{x}_i, \quad \mathbf{P}_i \in \mathbb{C}^{a_i \times a_i}, \quad i = 1, \dots, N-1.$$

To keep the transmitted power unchanged after precoding, the precoder matrices are restricted as:

$$\text{tr} \{ \mathbf{P}_i \mathbf{R}_{\mathbf{x}_i} \mathbf{P}_i^H \} \leq \text{tr} \{ \mathbf{R}_{\mathbf{x}_i} \}, \quad i = 0, \dots, N-1, \quad (16)$$

such that they satisfy the per-node long-term average power constraint:

$$\begin{aligned} \text{tr} \{ \mathbf{R}_{\bar{\mathbf{x}}_i} \} &= \text{tr} \{ \mathbb{E} \{ \bar{\mathbf{x}}_i \bar{\mathbf{x}}_i^H \} \} = \text{tr} \{ \mathbf{P}_i \mathbf{R}_{\mathbf{x}_i} \mathbf{P}_i^H \} \\ &\leq \text{tr} \{ \mathbf{R}_{\mathbf{x}_i} \} = \text{tr} \{ \mathbb{E} \{ \mathbf{x}_i \mathbf{x}_i^H \} \}. \end{aligned} \quad (17)$$

The received signal at the destination is given by:

$$\bar{\mathbf{y}}_N = \bar{\mathbf{G}}_N \mathbf{x}_0 + \bar{\mathbf{n}}, \quad (18)$$

where

$$\bar{\mathbf{G}}_N = \mathbf{H}_N \mathbf{P}_{N-1} \mathbf{H}_{N-1} \mathbf{P}_{N-2} \dots \mathbf{H}_2 \mathbf{P}_1 \mathbf{H}_1 \mathbf{P}_0 \quad (19)$$

is the end-to-end equivalent channel, and:

$$\begin{aligned} \bar{\mathbf{n}} &= \mathbf{n}_N \\ &+ \mathbf{H}_N \mathbf{P}_{N-1} \mathbf{n}_{N-1} \\ &+ \mathbf{H}_N \mathbf{P}_{N-1} \mathbf{H}_{N-1} \mathbf{P}_{N-2} \mathbf{n}_{N-2} \\ &+ \dots \\ &+ \mathbf{H}_N \mathbf{P}_{N-1} \mathbf{H}_{N-1} \dots \mathbf{H}_3 \mathbf{P}_2 \mathbf{n}_2 \\ &+ \mathbf{H}_N \mathbf{P}_{N-1} \mathbf{H}_{N-1} \dots \mathbf{H}_3 \mathbf{P}_2 \mathbf{H}_2 \mathbf{P}_1 \mathbf{n}_1 \end{aligned} \quad (20)$$

is the end-to-end equivalent colored noise. The noise covariance matrix is calculated as:

$$\begin{aligned} \mathbf{R}_{\bar{\mathbf{n}}} &= \mathbb{E} \{ \bar{\mathbf{n}} \bar{\mathbf{n}}^H \} \\ &= \mathbf{R}_N \\ &+ \mathbf{H}_N \mathbf{P}_{N-1} \mathbf{R}_{N-1} \mathbf{P}_{N-1}^H \mathbf{H}_N^H \\ &+ \mathbf{H}_N \mathbf{P}_{N-1} \mathbf{H}_{N-1} \mathbf{P}_{N-2} \mathbf{R}_{N-2} \mathbf{P}_{N-2}^H \mathbf{H}_{N-1}^H \mathbf{P}_{N-1}^H \mathbf{H}_N^H \\ &+ \dots \\ &+ \mathbf{H}_N \mathbf{P}_{N-1} \mathbf{H}_{N-1} \dots \mathbf{H}_3 \mathbf{P}_2 \mathbf{R}_2 \mathbf{P}_2^H \mathbf{H}_3^H \dots \mathbf{H}_{N-1}^H \mathbf{P}_{N-1}^H \mathbf{H}_N^H \\ &+ \mathbf{H}_N \mathbf{P}_{N-1} \mathbf{H}_{N-1} \dots \mathbf{H}_3 \mathbf{P}_2 \mathbf{H}_2 \mathbf{P}_1 \mathbf{R}_1 \mathbf{P}_1^H \mathbf{H}_2^H \mathbf{P}_2^H \mathbf{H}_3^H \dots \\ &\times \mathbf{H}_{N-1}^H \mathbf{P}_{N-1}^H \mathbf{H}_N^H. \end{aligned} \quad (21)$$

By Theorem 3 and Theorem 4 in the Appendix, the instantaneous end-to-end mutual information between the system input \mathbf{x}_0 and the system output $\bar{\mathbf{y}}_N$ is given by:

$$\begin{aligned} \mathcal{I}(\mathbf{x}_0; \bar{\mathbf{y}}_N) &= \mathcal{H}(\mathbf{x}_0) - \mathcal{H}(\mathbf{x}_0 | \bar{\mathbf{y}}_N) \\ &= \log \det(\pi e \mathbf{R}_{\mathbf{x}_0}) \\ &\quad - \log \det \left[\pi e \left(\mathbf{R}_{\mathbf{x}_0} - \mathbf{R}_{\bar{\mathbf{y}}_N \mathbf{x}_0}^T \mathbf{R}_{\bar{\mathbf{y}}_N}^{-1} \mathbf{R}_{\bar{\mathbf{y}}_N \mathbf{x}_0} \right) \right] \\ &= \log \det \left(\mathbf{I} + \mathbf{R}_{\mathbf{x}_0} \bar{\mathbf{G}}_N^H \mathbf{R}_{\bar{\mathbf{n}}}^{-1} \bar{\mathbf{G}}_N \right). \end{aligned} \quad (22)$$

For $i = 1, \dots, N$, the capacity of the system is

$$\begin{aligned} C &= \max_{\mathbf{P}_{i-1}} \log \det \left(\mathbf{I} + \mathbf{R}_{\mathbf{x}_0} \bar{\mathbf{G}}_N^H \mathbf{R}_{\bar{\mathbf{n}}}^{-1} \bar{\mathbf{G}}_N \right) \\ \text{s.t.} \quad &\text{tr} \{ \mathbf{P}_{i-1} \mathbf{R}_{\mathbf{x}_{i-1}} \mathbf{P}_{i-1}^H \} \leq \text{tr} \{ \mathbf{R}_{\mathbf{x}_{i-1}} \}. \end{aligned} \quad (23)$$

The maximum is taken over all possible precoding matrices \mathbf{P}_{i-1} , $i = 1, \dots, N$. The design problem is how to obtain the optimal set of precoding matrices \mathbf{P}_{i-1} to maximize the mutual information and consequently attain the channel capacity (Equation 23) of the correlated MIMO multi-hop wireless channel.

3.2 Asymptotic capacity and precoder design to maximize the individual mutual information

Since the objective function in Equation 23 is very complicated and neither a convex nor a concave function with respect to the to-be-designed variables \mathbf{P}_{i-1} , generally obtaining the optimal solution in closed form to this problem is impossible. In this section, we propose to relax

the objective function to obtain an asymptotic solution in closed form.

Instead of maximizing only the end-to-end mutual information between the source and the destination, we propose to maximize the individual mutual information between the transmitted signal and received signal at all hops. Based on each maximization problem at each hop, one after the others, each precoding matrix is designed.

Similarly to single-hop wireless models, it can be seen that the input-output relationship at each hop can be expressed as:

$$\mathbf{x}_i = \mathbf{H}_i \bar{\mathbf{x}}_{i-1} + \mathbf{n}_i = \mathbf{H}_i \mathbf{P}_{i-1} \mathbf{x}_{i-1} + \mathbf{n}_i, i = 1, \dots, N. \quad (24)$$

Note that we have the fundamental condition [37] $\det(\mathbf{I} + \mathbf{XY}) = \det(\mathbf{I} + \mathbf{YX})$. By Theorem 3 and Theorem 4 in the Appendix, the mutual information between the system input \mathbf{x}_{i-1} and the system output \mathbf{x}_i at the i -th hop is given by:

$$\begin{aligned} \mathcal{I}(\mathbf{x}_{i-1}; \mathbf{x}_i) &= \log \det \left(\mathbf{I} + \mathbf{R}_{x_{i-1}} \mathbf{P}_{i-1}^H \mathbf{H}_i^H \mathbf{R}_i^{-1} \mathbf{H}_i \mathbf{P}_{i-1} \right) \\ &= \log \det \left(\mathbf{I} + \mathbf{P}_{i-1} \mathbf{R}_{x_{i-1}} \mathbf{P}_{i-1}^H \mathbf{H}_i^H \mathbf{R}_i^{-1} \mathbf{H}_i \right). \end{aligned} \quad (25)$$

The precoding matrices \mathbf{P}_{i-1} , $i = 1, \dots, N$ are obtained by solving the maximization problems:

$$\begin{aligned} \max_{\mathbf{P}_{i-1}} \quad & \log \det \left(\mathbf{I} + \mathbf{P}_{i-1} \mathbf{R}_{x_{i-1}} \mathbf{P}_{i-1}^H \mathbf{H}_i^H \mathbf{R}_i^{-1} \mathbf{H}_i \right) \\ \text{s.t.} \quad & \text{tr} \{ \mathbf{P}_{i-1} \mathbf{R}_{x_{i-1}} \mathbf{P}_{i-1}^H \} \leq \text{tr} \{ \mathbf{R}_{x_{i-1}} \}. \end{aligned} \quad (26)$$

For $i = 1$, the maximization problem (26) becomes:

$$\begin{aligned} \max_{\mathbf{P}_0, \text{tr} \{ \mathbf{P}_0 \mathbf{R}_{x_0} \mathbf{P}_0^H \} \leq \text{tr} \{ \mathbf{R}_{x_0} \}} \quad & \log \det \left(\mathbf{I} + \mathbf{P}_0 \mathbf{R}_{x_0} \mathbf{P}_0^H \mathbf{H}_1^H \mathbf{R}_1^{-1} \mathbf{H}_1 \right). \end{aligned} \quad (27)$$

As \mathbf{R}_1^{-1} is definite and \mathbf{R}_{x_0} is semi-definite, let $\mathbf{P} = \mathbf{H}_1^H \mathbf{R}_1^{-1} \mathbf{H}_1 > 0$ and make the variable change $\mathbf{Q} = \mathbf{P}_0 \mathbf{R}_{x_0} \mathbf{P}_0^H \geq 0$, Equation 27 can be written as:

$$\max_{\mathbf{Q} \geq 0, \text{tr}(\mathbf{Q}) \leq \text{tr}(\mathbf{R}_{x_0})} \log \det(\mathbf{I} + \mathbf{QP}), \quad (28)$$

where its optimal solution \mathbf{Q} can be obtained in closed form by Theorem 1. It can be seen that the variable change $\mathbf{Q} = \mathbf{P}_0 \mathbf{R}_{x_0} \mathbf{P}_0^H \geq 0$ is legal as for every known matrix \mathbf{Q} , one can easily find out a corresponding matrix $\mathbf{P}_0 = \mathbf{Q}^{1/2} \mathbf{R}_{x_0}^{-1/2}$.

From the optimal value of \mathbf{Q} , it is obvious to have the optimal value of \mathbf{P}_0 since \mathbf{R}_{x_0} is semi-definite. After having the optimal value of \mathbf{P}_0 , from Equation 24, the covariance matrix \mathbf{R}_{x_1} can be calculated easily. It is also obvious to see that \mathbf{R}_{x_1} is semi-definite. Consequently, by using the optimal precoding matrices in the previous hops, the precoding matrix \mathbf{P}_{i-1} , $i = 2, \dots, N$ in the current i -th hop

can be optimally obtained by solving the maximization problems:

$$\max_{\bar{\mathbf{Q}} \geq 0, \text{tr}(\bar{\mathbf{Q}}) \leq \bar{\mathbf{P}}} \log \det(\mathbf{I} + \bar{\mathbf{Q}}\bar{\mathbf{P}}), \quad (29)$$

where $\bar{\mathbf{Q}} = \mathbf{P}_{i-1} \mathbf{R}_{x_{i-1}} \mathbf{P}_{i-1}^H \geq 0$ and $\bar{\mathbf{P}} = \mathbf{H}_i^H \mathbf{R}_i^{-1} \mathbf{H}_i > 0$, $\bar{\mathbf{P}} = \text{tr} \{ \mathbf{R}_{x_{i-1}} \}$.

3.3 Precoding design to minimize the detection error

When designing a wireless system, one criterion which is usually used for this purpose is the minimization of the detection error. To detect the source signal \mathbf{x}_0 from the received signal in Equation 18, the minimum mean square error (MMSE) estimator of \mathbf{x}_0 is [41]:

$$\tilde{\mathbf{x}}_0 = \left\{ \mathbf{R}_{x_0}^{-1} + \bar{\mathbf{G}}_N^H \mathbf{R}_N^{-1} \bar{\mathbf{G}}_N \right\}^{-1} \bar{\mathbf{G}}_N^H \mathbf{R}_N^{-1} \bar{\mathbf{y}}_N.$$

In essence, $\tilde{\mathbf{x}}_0$ is a *soft* estimate of the data vector \mathbf{x}_0 . The final *hard* decision $\hat{\mathbf{x}}_0$ is obtained by appropriately rounding up each element of $\tilde{\mathbf{x}}_0$ to the nearest signal point in the constellation. The mean square error (MSE) in the MMSE estimation of the source symbols from the received signal at the destination is given by [41]:

$$\text{tr} \left\{ \mathbf{R}_{x_0}^{-1} + \bar{\mathbf{G}}_N^H \mathbf{R}_N^{-1} \bar{\mathbf{G}}_N \right\}^{-1}. \quad (30)$$

In order to improve the detection performance, instead of designing the precoding matrices \mathbf{P}_{i-1} , $i = 1 \dots, N$ to maximize the end-to-end mutual information as shown in the above sections, we now design the precoding matrices \mathbf{P}_{i-1} to minimize the MSE (Equation 30) under the power constraint in Equation 16.

$$\begin{aligned} \min_{\mathbf{P}_{i-1}} \quad & \text{tr} \left\{ \mathbf{R}_{x_0}^{-1} + \bar{\mathbf{G}}_N^H \mathbf{R}_N^{-1} \bar{\mathbf{G}}_N \right\}^{-1} \\ \text{s.t.} \quad & \text{tr} \{ \mathbf{P}_{i-1} \mathbf{R}_{x_{i-1}} \mathbf{P}_{i-1}^H \} \leq \text{tr} \{ \mathbf{R}_{x_{i-1}} \}. \end{aligned} \quad (31)$$

Similar to the design for mutual information maximization, it can be seen that the objective function in Equation 31 is very complicated and neither a convex nor a concave function with respect to the to-be-designed variables \mathbf{P}_{i-1} . Since it is impossible to obtain the optimal solution in closed form for Problem (31), we relax the optimization problem (31) for an asymptotic solution in closed form.

Instead of globally minimizing the MSE of the source symbol detection at the destination only, we minimize the MSE of the soft estimate at each hop. Based on each minimization problem at each hop, each precoding matrix is obtained, one after the others. The input-output relationship (Equation 24) at each hop is again used for the asymptotic design. The MSE in the MMSE estimation of the transmitted signal \mathbf{x}_{i-1} from the received signal \mathbf{x}_i in Equation 24 is:

$$\text{tr} \left\{ \mathbf{R}_{x_{i-1}}^{-1} + \mathbf{P}_{i-1}^H \mathbf{H}_i^H \mathbf{R}_i^{-1} \mathbf{H}_i \mathbf{P}_{i-1} \right\}^{-1}, i = 1, \dots, N. \quad (32)$$

The precoding matrices \mathbf{P}_{i-1} are obtained by solving the minimization problems:

$$\begin{aligned} \min_{\mathbf{P}_{i-1}} \quad & \text{tr} \left\{ \mathbf{R}_{x_{i-1}}^{-1} + \mathbf{P}_{i-1}^H \mathbf{H}_i^H \mathbf{R}_i^{-1} \mathbf{H}_i \mathbf{P}_{i-1} \right\}^{-1} \\ \text{s.t.} \quad & \text{tr} \left\{ \mathbf{P}_{i-1} \mathbf{R}_{x_{i-1}} \mathbf{P}_{i-1}^H \right\} \leq \text{tr} \left\{ \mathbf{R}_{x_{i-1}} \right\}. \end{aligned} \quad (33)$$

Let $\mathbf{Q}_i = \mathbf{H}_i^H \mathbf{R}_i^{-1} \mathbf{H}_i \geq 0$, the optimization problem can be stated as:

$$\begin{aligned} \min_{\mathbf{P}_{i-1}} \quad & \text{tr} \left\{ \mathbf{R}_{x_{i-1}}^{-1} + \mathbf{P}_{i-1}^H \mathbf{Q}_i \mathbf{P}_{i-1} \right\}^{-1} \\ \text{s.t.} \quad & \text{tr} \left\{ \mathbf{P}_{i-1} \mathbf{R}_{x_{i-1}} \mathbf{P}_{i-1}^H \right\} \leq \text{tr} \left\{ \mathbf{R}_{x_{i-1}} \right\}. \end{aligned} \quad (34)$$

This optimization problem has the same form and solution as those in [19], Equation 12. The optimal solution is summarized in the following.

Let M be the rank of \mathbf{Q}_i . Make the following SVDs of $\mathbf{Q}_i = \mathbf{U}_Q^H \Sigma_Q \mathbf{U}_Q$ and $\mathbf{R}_{x_{i-1}} = \mathbf{U}_{x_{i-1}}^H \Sigma_{x_{i-1}} \mathbf{U}_{x_{i-1}}$. Here, $\Sigma_Q = \text{diag} \left[\Sigma_{MQ}^2, \mathbf{0} \right]$, with $\Sigma_{MQ} > 0$, is a diagonal matrix having the eigenvalues of \mathbf{Q}_i on its main diagonal in decreasing order and \mathbf{U}_Q is the unitary matrix whose columns are the corresponding eigenvectors of \mathbf{Q}_i . Analogously, $\Sigma_{x_{i-1}} > 0$ is the diagonal matrix having the eigenvalues of $\mathbf{R}_{x_{i-1}}$ in decreasing order on its main diagonal, and $\mathbf{U}_{x_{i-1}}$ is the unitary matrix whose columns are the corresponding eigenvectors.

Theorem 2. The optimal precoder matrices \mathbf{P}_{i-1} to be used with the MMSE detection at each hop are:

$$\mathbf{P}_{i-1} = \hat{\mathbf{U}}_Q^H \text{diag} \left\{ \left[\left(\frac{\bar{\mu}^{-1/2}}{\gamma(j)} - \frac{1}{\gamma^2(j)} \right)^+ \right]^{1/2} \right\}_{j=1, \dots, M} \hat{\mathbf{U}}_{x_{i-1}},$$

where $\gamma(j) = \Sigma_{x_{i-1}}^{1/2}(j, j) \Sigma_{MQ}(j, j)$, $\hat{\mathbf{U}}_Q$ and $\hat{\mathbf{U}}_{x_{i-1}} \in \mathbb{C}^{M \times N}$ with $\mathbf{U}_Q = [\hat{\mathbf{U}}_Q^H *]^H$, $\mathbf{U}_{x_{i-1}} = [\hat{\mathbf{U}}_{x_{i-1}}^H *]^H$, and $\bar{\mu}$ is chosen such that $\sum_{j=1}^M \Sigma_{MQ}^{-2}(j, j) (\bar{\mu}^{-1/2} \gamma(j) - 1)^+ = \text{tr} \{ \mathbf{R}_{x_{i-1}} \}$.

4 Simulation results

This section provides simulation results to illustrate the performance of the proposed designs. In all simulation results presented in this section, colored noise is generated by multiplying a matrix \mathbf{G}_i with white noise vector \mathbf{w}_i [19], whose components are $\mathcal{CN}(0, \sigma_w^2)$. This means that the covariance matrix of colored noise is $\mathbf{R}_i = \sigma_w^2 \mathbf{G}_i \mathbf{G}_i^H$. To have the average power of colored noise the same as that of white noise, \mathbf{G}_i is chosen such that $\text{tr} \{ \mathbf{G}_i \mathbf{G}_i^H \} = a_i$, $i = 1, \dots, N$. The average transmitted power is chosen to be unity, the signal-to-noise ratio (SNR) in dB is defined as $\text{SNR} = -10 \log_{10} \sigma_w^2$, and the average noise power can be calculated as $\sigma_w^2 = 10^{-\text{SNR}/10}$.

The wireless channel model is assumed to be quasi-static block fading and spatially correlated by the Kronecker model with $\sigma_{hi}^2 = 1$. The one-ring model in

([13], Equation 6) is used to generate the elements of the covariance matrices Σ_{ri} and Σ_{ti} . Specifically, $\Sigma_{ti}(n, m) \approx J_0 \left(\Delta_{ti} \frac{2\pi}{\lambda} d_{ti} |m - n| \right)$, $m, n = 1, \dots, a_{i-1}$, and $\Sigma_{ri}(u, v) \approx J_0 \left(\Delta_{ri} \frac{2\pi}{\lambda} d_{ri} |u - v| \right)$, $u, v = 1, \dots, a_i$. Here, we chosen $\Delta_{ti} = 5\pi i/180$ and $\Delta_{ri} = 10\pi i/180$ are the angle spreads (in radian) of the transmitter and the receiver at the i -th hop; $d_{ti} = 0.5\lambda$ and $d_{ri} = 0.3\lambda$ are the spacings of the transmitting and receiving antenna arrays at the i -th hop; λ is the wavelength and $J_0(\cdot)$ is the zeroth-order Bessel function of the first kind. Note that the angle spreads, Δ_{ti} and Δ_{ri} , the wavelength λ , and the antenna spacings, d_{ti} and d_{ri} , determine how correlated the fading is at the transmitting and receiving antenna arrays at each hop.

Figure 3 presents the mutual information of correlated four-hop wireless channels under colored noise with ideal channel state information at the transmitters (CSIT) when having 2×2 and 4×4 MIMO antennas. We used ‘SeDuMi’ [38] solver for the numerically optimal solution. It can be observed that the closed-form solution and the numerical solution yield the same optimal mutual information value.

Figure 4 shows the mutual information of two-hop wireless 2×2 MIMO channels under colored noise in three cases: 1) the upper bound of the average end-to-end mutual information with the asymptotic design solution obtained from Section 2.3, 2) the average end-to-end mutual information with the asymptotic design, and 3) the average end-to-end mutual information with the optimal design solution obtained from the numerical interior-point-method. It can be seen in Figure 4 that the average end-to-end mutual information with asymptotic design is very closed to that obtained by the numerical interior point method. However, these mutual information values are less than and closed to the upper bound of the mutual information obtained by the asymptotic

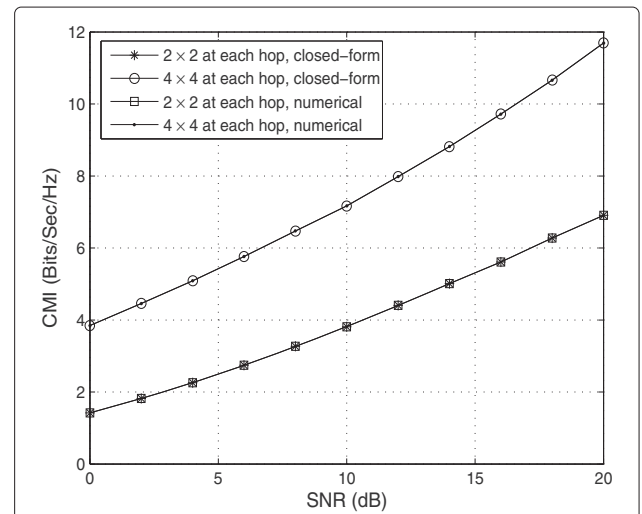


Figure 3 Comparison of mutual information for correlated four-hop MIMO channels under colored noise with ideal CSIT.

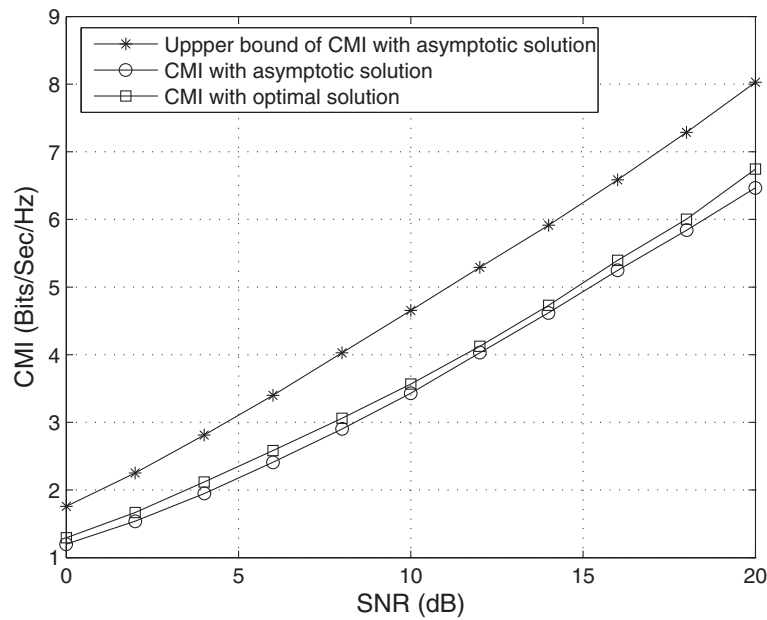


Figure 4 Comparison of average mutual information for a correlated four-hop MIMO channel under colored noise with only the channel statistics at the transmitters.

solution. It verifies that the asymptotic design can efficiently yield an acceptable mutual information while saving a huge computational complexity compared to the numerical design, especially when the system size is large.

When precoding technique is applied, the wireless channel model has 4×4 MIMO antennas, and the vector \mathbf{x}_0 of a_0 correlated source symbols are generated as $\mathbf{x}_0 = \mathbf{G}_s \mathbf{s}_0$, where \mathbf{s}_0 is a length- a_0 vector of uncorrelated symbols drawn from the Gray-mapped quadrature phase-shift keying (QPSK) constellation of unit energy. The matrix \mathbf{G}_s is generated arbitrarily but normalized such that $\mathbf{G}_s \mathbf{G}_s^H$ has unit elements on the diagonal. This ensures the same transmitted power as in the case of uncorrelated data symbols. Note that the correlation matrix of the source symbols is $\mathbf{R}_{x_0} = \mathbf{G}_s \mathbf{G}_s^H$.

Figures 5, 6, and 7 present the end-to-end mutual information values of correlated wireless MIMO channels having correlated source symbols under colored noise in four cases: 1) with the precoding design in Section 3.2 to maximize the individual mutual information, 2) with the precoding design in Section 3.3 to minimize the individual soft detection error, 3) with the precoding design in ([27], Section V-C), and 4) without the precoding techniques.

In Figure 5, the wireless channel under consideration has only one hop. In this single-hop scheme, the proposed design to maximize the mutual information is obviously optimal as the end-to-end mutual information is also the mutual information at the only hop. As expected, three systems having the precoding techniques perform better

than the system without being applied the precoding technique. It can be observed that the mutual information with the precoding design to maximize the mutual information is better than that of the precoding design to minimize the soft detection error. However, the more important observation is that both the end-to-end mutual information values of the wireless systems having the proposed precoding designs are larger than the mutual information value of the design in ([27], Section V-C). This performance gain is reasonable as the design in ([27], Section V-C) only proposed optimal precoding directions with equal power allocation, while in our designs two precoding problems of transmitted power allocation and transmitted signal direction are optimally designed at each hop.

In Figure 6, the simulation results for the two-hop wireless MIMO channels are illustrated. In this two-hop scheme, although the end-to-end mutual information values of the wireless systems having the proposed precoding designs are better than that of the wireless system having the precoding design in ([27], Section V-C), it is very interesting that the precoding design to minimize the soft detection error gives a better capacity performance than that of the precoding design to maximize the mutual information.

When the wireless channels have four hops, as shown in Figure 7, the precoding design to minimize the individual soft detection error yields a significant performance gain than that of the design to maximize the individual mutual information value. It is also depicted in Figure 7 that

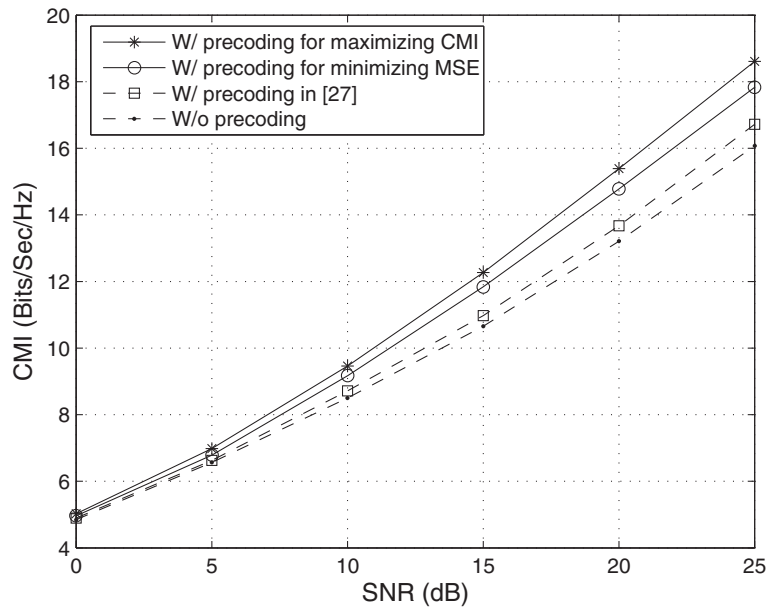


Figure 5 Comparison of end-to-end mutual information for correlated wireless single-hop MIMO channels with and without precoding techniques.

all the proposed precoding designs for four-hop wireless channels have a better performance than that of the system without the precoding technique.

5 Conclusions

In this paper, the closed-form source symbol covariance is designed to maximize the mutual information between the channel input and the channel output of

correlated wireless multi-hop MIMO systems when having the full knowledge of channel at the transmitters. When having only channel statistics at the transmitters, the numerically optimal source symbol covariance and a sub-optimal source symbol covariance in closed form are designed to maximize the average end-to-end mutual information. Moreover, two sets of precoding matrices are sub-optimally designed for generally correlated multi-hop

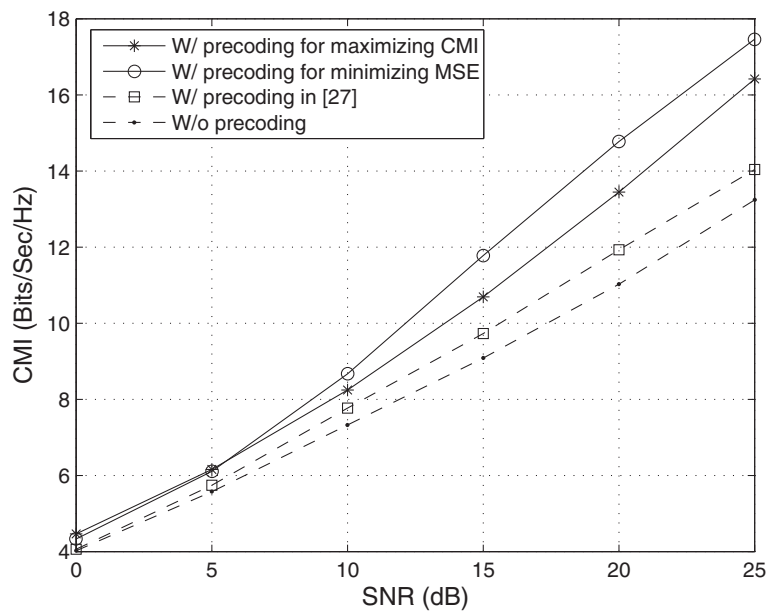


Figure 6 Comparison of end-to-end mutual information for correlated wireless two-hop MIMO channels with and without precoding techniques.

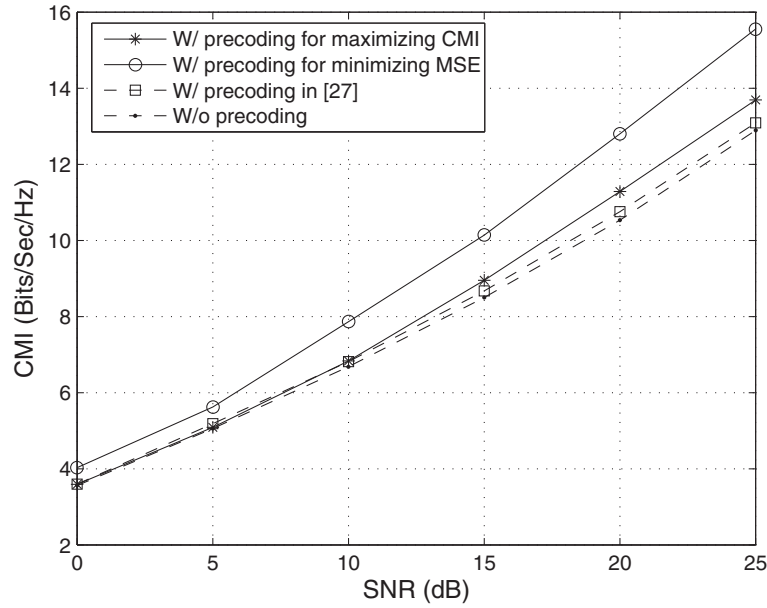


Figure 7 Comparison of end-to-end mutual information for correlated wireless four-hop MIMO channels with and without precoding techniques.

MIMO channels. The first design is obtained by maximizing the mutual information between the input and output signals at each hop while the second design is obtained by minimizing the MSE of the soft detection at each hop. Simulation results show that the proposed precoding designs significantly increase the end-to-end mutual information of the wireless system, while it does not spend system resources such as transmission power or bandwidth.

Appendix

Theorem 3. ([42], p. 522) Suppose that \mathbf{y} and \mathbf{x} are two random variables of zero mean with the covariance matrix:

$$\mathbf{R}_{x,y} = \begin{bmatrix} \mathbf{R}_y & \mathbf{R}_{yx} \\ \mathbf{R}_{yx}^T & \mathbf{R}_x \end{bmatrix} = \begin{bmatrix} E\{\mathbf{y}\mathbf{y}^H\} & E\{\mathbf{y}\mathbf{x}^H\} \\ E\{\mathbf{x}\mathbf{y}^H\} & E\{\mathbf{x}\mathbf{x}^H\} \end{bmatrix}$$

Then, the conditional distribution $\mathbf{x}|\mathbf{y}$ has the covariance:

$$\mathbf{R}_{x_0} - \mathbf{R}_{yx}^T \mathbf{R}_y^\dagger \mathbf{R}_{yx}.$$

Here, \mathbf{R}_y^\dagger is the pseudo-inverse of \mathbf{R}_y .

Theorem 4. ([1], Lemma 2) For any zero-mean random vector \mathbf{x} with the covariance $E\{\mathbf{x}\mathbf{x}^H\} = \mathbf{R}_{x_0}$, the entropy [36] of \mathbf{x} satisfies:

$$\mathcal{H}(\mathbf{x}) \leq \log \det(\pi e \mathbf{R}_{x_0})$$

with equality if and only if \mathbf{x} is a circularly symmetric complex Gaussian random variable with zero mean and covariance \mathbf{R}_{x_0} , i.e., among the random variables with the

same mean and covariance, the Gaussian one gives the largest entropy.

Proof of Theorem 1. The function $F(\mathbf{Q}) = \log \det(\mathbf{I} + \mathbf{Q}\mathbf{P})$ is not readily spectral. However, we can deduce Equation 11 to spectral optimization by making the SVD of $\mathbf{P} = \mathbf{U}^H \mathbf{D}_p \mathbf{U}$ and changing the variable $\mathbf{X} = \sqrt{\mathbf{D}_p} \mathbf{U} \mathbf{Q} \mathbf{U}^H \sqrt{\mathbf{D}_p}$ in Equation 12, it can be seen that $\text{tr}(\mathbf{Q}) = \text{tr}(\mathbf{U}^H \mathbf{D}_p^{-1/2} \mathbf{X} \mathbf{D}_p^{-1/2} \mathbf{U}) = \text{tr}(\mathbf{D}_p^{-1} \mathbf{X})$. Therefore, the optimization problem (12) is now expressed as follows:

$$\max_{\mathbf{X} \geq 0, \text{tr}(\mathbf{D}_p^{-1} \mathbf{X}) \leq P} \log \det(\mathbf{I} + \mathbf{X}) \quad (35)$$

where the function $\mathbf{X} \rightarrow \log \det(\mathbf{I} + \mathbf{X})$ is spectral and the function $\mathbf{X} \rightarrow \text{Trace}(\mathbf{D}_p^{-1} \mathbf{X})$ is linear and thus differentiable. According to [43]:

$$\begin{aligned} [\log \det(\mathbf{I} + \mathbf{X})]' &= \mathbf{V}^H (\mathbf{I} + \mathbf{D}_X)^{-1} \mathbf{V} = (\mathbf{I} + \mathbf{X})^{-1}, \\ [\text{Trace}(\mathbf{D}_p^{-1} \mathbf{X})]' &= \mathbf{D}_p^{-1}, \end{aligned}$$

where $\mathbf{X} = \mathbf{V}^H \mathbf{D}_X \mathbf{V}$ by SVD.

For simplicity, we relax the constraint $\mathbf{X} \geq 0$ in Equation 35 by $X_{ii} \geq 0$, i.e., instead of Equation 35 we consider:

$$\max_{X_{ii} \geq 0, \text{Tr}(\mathbf{D}_p^{-1} \mathbf{X}) \leq P} \log \det(\mathbf{I} + \mathbf{X}). \quad (36)$$

In the next few lines, we will prove that the optimal solution \mathbf{X} is an diagonal matrix so Equations 35 and 36 have

the same optimal solution. The Lagrangian of Equation 36 is:

$$\begin{aligned}\mathcal{L}(\mathbf{X}, \alpha, \mu) = & -\log \det(\mathbf{I} + \mathbf{X}) - \text{Trace}(\mathbf{X}\mathbf{D}_\alpha) \\ & + \mu(\text{Trace}(\mathbf{D}_p^{-1}\mathbf{X}) - P), \\ \alpha_i \geq 0, \mu \geq 0, \mathbf{D}_\alpha = & \text{diag}(\alpha)\end{aligned}$$

Since $\log \det(\mathbf{I} + \mathbf{X})$ is concave and $-\log \det(\mathbf{I} + \mathbf{X})$ is convex so Equation 36 is a convex programming. According to the Karush-Kuhn-Tucker (KKT) condition [44] for the optimality of convex programming, the optimal solution to the optimization problem in Equation 36 and the corresponding Lagrange multipliers must satisfy the following necessary and sufficient conditions:

$$0 = \frac{\partial \mathcal{L}(\alpha, \mu)}{\partial \mathbf{X}} = -(\mathbf{I} + \mathbf{X})^{-1} - \mathbf{D}_\alpha + \mu \mathbf{D}_p^{-1}, \quad (37)$$

$$0 = \alpha_i X_{ii}, \quad i = 1, 2, \dots, n; \quad 0 = \mu(\text{Trace}(\mathbf{D}_p^{-1}\mathbf{X}) - P). \quad (38)$$

From Equation 37, it is clear that \mathbf{X} is diagonal, and therefore, Equations 35 and 36 are equivalent. Solving Equations 37 and 38 gives the following water-filling solution:

$$D_p^{-1}(i, i)X(i, i) = (\mu^{-1} - D_p^{-1}(i, i))^+ \quad (39)$$

where $x^+ = \max\{0, x\}$ and μ is chosen such that $\text{Trace}(\mathbf{D}_p^{-1}\mathbf{X}) = P$. The optimal solution is $\mathbf{Q} = \mathbf{U}^H (\mathbf{D}_p^{-1/2} \mathbf{X} \mathbf{D}_p^{-1/2}) \mathbf{U} = \mathbf{U}^H \mathbf{D}_p^{-1} \mathbf{X} \mathbf{U}$.

Competing interests

The authors declare that they have no competing interests.

Acknowledgements

This research is funded by Vietnam National Foundation for Science and Technology Development (NAFOSTED) under grant number 102.02-2012.28.

Author details

¹ Faculty of Electronics and Telecommunications, University of Science, Vietnam National University, Ho Chi Minh City, Vietnam. ² Department of Computer and Electronics Engineering, University of Nebraska-Lincoln, Omaha NE 68182, USA. ³ School of Engineering, Tan Tao University, Tan Duc E-city, Duc Hoa, Long An, Vietnam.

Received: 7 September 2014 Accepted: 5 April 2015

Published online: 03 May 2015

References

- IE Telatar, Capacity of multi-antenna Gaussian channels. *Eur Trans. Tele.* **10**, 585–595 (1999)
- IS Association. IEEE 802.11: Wireless LAN medium access control (MAC) and physical layer (PHY) specifications, 2007 edition. <http://standards.ieee.org/getieee802/download/802.11-2007.pdf>, 2007
- Linksys, Linksys WRT54G. <http://www.speedguide.net/broadband-view.php?hw=36>, 2006
- 3GPP TSG RAN TR 25.848 v4.0.0, Physical Layer Aspects of UTRA High Speed Downlink Packet Access (release 4) (2004)
- 3GPP2 TSG C.S0002-C v1.0 Physical Layer Standard for cdma2000 Spread Spectrum Systems (1999)
- A Doufexi, S Armour, M Butler, A Nix, D Bull, J McGeehan, P Karlsson, A comparison of the HIPERLAN/2 and IEEE 802.11a wireless LAN standards. *IEEE Commun. Mag.* **40**, 172–80 (2002)
- IEEE Std 802.16g, Local and Metropolitan Area Networks Part 16: Air Interface for Fixed Broadband Wireless Access Systems (2002)
- JP Kermaol, L Schumacher, PE Mogensen, KI Pedersen, in *Proc. IEEE Veh. Technol. Conf. (VTC-Fall)*. Experimental investigation of correlation properties of MIMO radio channels for indoor picocell scenario, (2000), pp. 14–21
- H Bolcskei, D Gesbert, AJ Paulraj, On the capacity of OFDM-based spatial multiplexing systems. *IEEE Trans. Commun.* **50**, 225–234 (2002)
- H Zhang, Y Li, A Reid, J Terry, Optimum training symbol design for MIMO OFDM in correlated fading channels. *IEEE Trans. Wireless Commun.* **5**, 2343–2347 (2006)
- H Bolcskei, M Borgmann, AJ Paulraj, Impact of the propagation environment on the performance of space-frequency coded MIMO-OFDM. *IEEE J. Selected Areas Commun.* **21**, 427–439 (2003)
- M Enescu, T Roman, V Koivunen, State-space approach to spatially correlated MIMO OFDM channel estimation. *Signal Process. ScienceDirect.* **87**, 2272–2279 (2007)
- D Shiu, G Foschini, M Gans, J Kahn, Fading correlation and its effect on the capacity of multielement antenna systems. *IEEE Trans. Commun.* **48**, 502–513 (2002)
- I Akyildiz, X Wang, A survey on wireless mesh networks. *IEEE Commun. Magazine.* **43**, S23–S30 (2005)
- K Shi, E Serpedin, P Cibat, Decision-directed fine synchronization in OFDM systems. *IEEE Trans. Commun.* **53**, 408–412 (2005)
- T Wong, B Park, Training sequence optimization in MIMO systems with colored interference. *IEEE Trans. Commun.* **12**, 1939–1947 (2004)
- YP Lin, S Phong, Optimal ISI-Free DMT transceiver for distorted channels with colored noise. *IEEE Trans. Signal Process.* **49**, 2702–2712 (2001)
- CD Richmond, Mean-squared error and threshold SNR prediction of maximum-likelihood signal parameter estimation with estimated colored noise covariances. *IEEE Trans. Inf. Theory.* **52**, 2146–2164 (2006)
- NN Tran, HD Tuan, HH Nguyen, Training signal and precoder designs for OFDM under colored noise. *IEEE Trans. Veh. Technol.* **57**, 3911–3917 (2008)
- S Jafar, S Vishwanath, A Goldsmith, in *Proc. Inter. Conf. Commun. (ICC)*. Channel capacity and beamforming for multiple transmit and receive antennas with covariance feedback, (2001), pp. 2266–2270
- A Goldsmith, *Wireless Communications*. (Cambridge, University press, 2005)
- SL Loyka, Channel capacity of two-antenna BLAST architecture. *Electron. Letter.* **35**, 1421–1422 (1999)
- B Wang, J Zhang, A Hst-Madsen, On the capacity of MIMO relay channels. *IEEE Trans. Inform. Theory.* **51**, 29–43 (2005)
- H Bolcskei, R Nabar, O Oyman, A Paulraj, Capacity scaling laws in MIMO relay networks. *IEEE Trans. Wireless Commun.* **5**, 1433–1444 (2006)
- S Borade, L Zheng, R Gallager, Amplify-and-forward in wireless relay networks: rate, diversity, and network size. *IEEE Trans. Inform. Theory.* **53**, 3302–3318 (2007)
- N Fawaz, K Zarifi, M Debbah, D Gesbert, in *IEEE ITW08, Information Theory Workshop*. Asymptotic capacity and optimal precoding strategy of multi-level precoder & forward in correlated channels, (2008), pp. 209–213
- N Fawaz, K Zarifi, M Debbah, D Gesbert, Asymptotic capacity and optimal precoding in MIMO multi-hop relay network. *IEEE Trans. Inform. Theory.* **57**, 2050–2069 (2011)
- Y Fan, JS Thompson, in *Proc. IEEE GLOBECOM 2005*. On the outage capacity of mimo multihop networks, (2005), pp. 2208–2213
- AI Sulyman, G Takahara, HS Hassanein, M Kousa, in *Proc. IEEE ICC 2009*. Multi-hop capacity of MIMO-multiplexing relaying in WiMAX Mesh networks, (2009), pp. 1–5
- AI Sulyman, G Takahara, HS Hassanein, M Kousa, Multi-hop capacity of MIMO-multiplexing relaying systems. *IEEE Trans. Wireless Commun.* **8**, 3095–3103 (2009)
- J Kermaol, L Schumacher, KI Pedersen, PE Mogensen, F Frederiksen, A stochastic MIMO radio channel model with experimental validation. *IEEE J. Selected Areas Commun.* **20**, 1211–1226 (2002)

32. K Yu, M Bengtsson, B Ottersten, D McNamara, P Karlsson, Modeling of wideband MIMO radio channels based on NLoS indoor measurements. *IEEE Trans. Veh. Technol.* **53**, 655–665 (2004)
33. JH Kotecha, AM Sayeed, Transmit signal design for optimal estimation of correlated MIMO channel. *IEEE Trans. Signal Process.* **52**, 546–557 (2004)
34. H Bolcskei, *Principles of MIMO-OFDM wireless systems*. CRC Handbook on Signal Processing for Communications. (M Ilnkahl, ed.), (2004). to appear, online at <http://www.nari.ee.ethz.ch/commth/pubs/p/crc03>
35. NN Tran, HD Tuan, HH Nguyen, Superimposed training designs for spatially correlated MIMO-OFDM systems. *IEEE Trans. Wireless Commun.* **53**, 876–880 (2010)
36. T Cover, J Thomas, *Elements of Information Theory*. (Wiley, New York, 1991)
37. RA Horn, CR Johnson, *Matrix Analysis*. (University Press, Cambridge, 1985)
38. O Romanko, I Pólik, T Terlaky, The homepage for SeDuMi. <http://sedumi.ie.lehigh.edu/>
39. KC Toh, MJ Todd, RH Tutuncu, SDPT3 version 4.0 (beta) - A MATLAB software for semidefinite-quadratic-linear programming. <http://www.math.nus.edu.sg/~mattohkc/sdpt3.html>
40. HR Bahrami, T Le-Ngoc, Precoder design based on correlation matrices for MIMO systems. *IEEE Trans. Wireless Commun.* **5**, 3579–3587 (2006)
41. SM Kay, *Fundamentals of Statistical Signal Processing*. (Prentice Hall PTR, New Jersey, 1993). vol. I - estimation theory
42. C Rao, *Linear Statistical Inference and its Applications*. (John Wiley and Sons, New Jersey, 1973)
43. A Lewis, Derivatives of spectral functions. *Math. Oper. Res.* **21**, 576–588 (1996)
44. D Luenberger, *Linear and Nonlinear Programming*. (Springer, New York, 2003)

Submit your manuscript to a SpringerOpen[®] journal and benefit from:

- Convenient online submission
- Rigorous peer review
- Immediate publication on acceptance
- Open access: articles freely available online
- High visibility within the field
- Retaining the copyright to your article

Submit your next manuscript at ► springeropen.com